Distribution, source identification, and ecological-health risks of potentially toxic elements (PTEs) in soil of thallium mine area (southwestern Guizhou, China)

Jiang, Feng; Ren, Bozhi; Hursthouse, Andrew; Deng, Ren-Jian; Wang, Zhenghua

Published in:
Environmental Science and Pollution Research

DOI:
10.1007/s11356-019-04997-3

Published: 01/06/2019

Document Version
Peer reviewed version

Distribution, Source Identification, and Ecological-health Risks of Potentially Toxic Elements (PTEs) in soils from a Thallium Mine Area Southwestern Guizhou, China

Abstract:

The exploitation of thallium (Tl) resources through mining poses a significant threat to ecological systems and human health due to its high toxicity and ready assimilation by human body. We report the first assessment of the pollution, spatial distribution, source and ecological-health risks of potentially toxic elements (PTEs) in Tl mining area of southwest Guizhou, China. Spatial distribution maps for PTEs were visualized by ArcGIS to identify their distribution trends. We use the enrichment factor (EF), correlation analysis and principal component analysis to identify likely sources of seven PTEs mining area. The wider risk assessment was evaluated using the geoaccumulation index (I_{geo}), potential ecological risk index (RI), human non-carcinogenic risk (HI) and carcinogenic risk (CR). The results revealed the PTEs content in the study area identifies direct mining, metal production and domestic pollution sources. In addition the distribution of PTEs was also affected by the topography, rain water leaching and river dispersals. The main elements of concern are Tl and As, while Cd, Cr, Cu, Pb and Zn do not show significant enrichment in the area despite associations with the ore deposit. Risk assessment identifies strong pollution and ecological risks, and poses unacceptable non-carcinogenic (HI) and carcinogenic risks (RI) to local residents, especially for children. The ecological risk in the study is identified to be predominantly from Tl (74.32%), followed by As (8.57%) and Cd (7.32%). The contribution of PTEs to the non-carcinogenic risk of humans in the study area is exclusively from As and Tl, while the carcinogenic risk is dominated by As, and the other elements pose no significant risk to human health.

Keywords: Thallium mine area; Potentially toxic elements (PTEs); Spatial distribution; Source identification; Ecological risk; Health risk

1. Introduction

A number of heavy metals and metalloids are potentially toxic elements (PTEs) persistent in the environment (Yuan et al. 2018). The pollution of the environment and toxicity to the wider ecosystem and for human beings continues to be a major concern in modern society (Stewart and Hursthouse 2018). PTEs are found in rocks and soils as trace elements in nature, but most of them are released into the environment by human activities (Karakus 2012). Such as industrial processing and mining activities (direct mining and smelting), transportation activities (automobile exhaust) and agricultural activities (fertilizers, pesticides, sludge and waste water) (Chen et al. 2018; Islam et al. 2015; Mcgrath and Lane 1989). For the terrestrial environment, the main impact from PTE pollution is to ultimately create wasteland, and for the aquatic environment, an excess of PTEs can inhibit the growth and reproduction of higher terrestrial and aquatic plants, algae and invertebrate. In addition, PTEs in soil can be ingested into human or animal body through the food chain, and can be continuously enriched and potential exposure and harm to human health (Azhari et al. 2017). The PTEs in soil can also be ingested directly through mouth, skin contact or breathing into the human body, adding to exposure and increasing risk (Sun et al. 2010). Long-term exposure to high levels of Cd can lead to lung cancer, prostate hyperplasia, renal dysfunction (Wu et al., 2018). Excessive intake of Pb can cause damage to nerves, bones, blood circulation, endocrine and immune systems (Pareja-Carrera et al., 2014; Pascaud

et al., 2014). Excessive intake of Cu affect liver and kidney function and central nervous system, induce depression and even lung cancer (Sani 2017). Therefore, it is of importance to understand the spatial distribution of PTEs in soil and evaluate its impact on the environment and risk to human health.

Environmental impacts associated with Tl contamination are relatively uncommon. However, Tl is a relatively toxic element with toxicity to mammals higher than Cd, Pb, Zn and other trace metals (Anagboso et al. 2013; Peter and Viraraghavan 2005; Zitko et al. 1975), and thallium is recognized as one of the thirteen priority metal pollutants in the world (Xiao et al. 2012). The consumption of Tl contaminated agricultural products is of concern. Ingestion of Tl can cause cardiovascular diseases and lead to acute poisoning of animals and plants (Peter and Viraraghavan 2005; Wappelhorst et al. 2000). Food crops grown in thallium contaminated areas can cause chronic thallium poisoning which is difficult to diagnose in the early stage and is easy to miss.(Liu et al. 2017a). The main symptoms of chronic thallium poisoning are neurological impairment, loss of vision, hair loss, and possible teratogenicity and mutagenicity. Siegel (1976) showed that thallium and potassium antagonizes each other in biological processes. Once thallium replaces potassium in the organism, plants will suffer great harm. In thallium contaminated soil, the growth of wheat is low, leaves are yellow and curly, and the yield per unit of soybean decreases (Kaplan et al. 1998). Microbes in soil are sensitive to thallium, which can inhibit the formation of nitrifying bacteria and cause adverse effects on agriculture (Chen et al. 2001). A large amount of thallium is released into the environment through various industrial activities, and the long-term accumulation of thallium will become a "chemical time bomb" of the future environment (Wang et al. 2007).

Although Tl is highly toxic, it is at low concentrations in soil and rare in nature. It is often ignored by researchers in ecological-health risk assessment, whilst in the past risk assessment, of PTEs has included Cd, Cr, Co, Cu, As, Pb, Hg, Zn and Ni (Azhari et al. 2017; Chen et al. 2018; Liu et al. 2019; Zhang et al. 2018), with very infrequent risk assessment for Tl. The low temperature epithermal deposits in Southwestern China (Xiao et al. 2012) have been identified as regions where enhanced baseline Tl occurs associated with mineralization and a number of potentially toxic elements, having potentially wider environmental impact. Despite this recent interest there are few detailed studies of environmental pollution and risk assessment related to Tl (Liang et al. 2017; Liu et al. 2017a). We report here an assessment of an independent Tl deposit from southwestern Guizhou Province, centered on Lanmuchang, a historic Tl-Hg deposit. Associated with this are coal mine and arsenic ore enrichment activities and a mining history of more than 300 years.

The main objectives of the study were to use this location to provide a relative assessment of this less well understood element and associated contaminants by : (1) evaluating the spatial distribution of PTEs in the soils of the area (Tl, As, Cd, Cr, Cu, Pb, Zn). (2) using statistical methods identify potential source contributions to pollutant loading. (3) evaluate the potential ecological and human health impact on local residents (4) assess the significance of data on recommendation for management of the site including remediation objectives in the wider mining area.

2. Materials and methods

2.1 Study area

The study area is located in Guizhou Province, Southwest China (105°30′23″E, 25°31′28″N) (Jia et al. 2013). The study area is a rural area of about 1000 inhabitants, with more than 400 people having been found to have been poisoned by Tl since the 1960s (Jia et al. 2013; Xiao et al. 2007, 2012). Economic development lags behind the regional average and poverty is widespread (Xiao et al. 2007).

The local population are permanent residents, and the land is mainly used for agriculture and habitation. The population is distributed in the vicinity of rivers and main roads (Xiao et al. 2007). The area has the characteristics of Karst landform, with an average elevation of 1400 meters and a fluctuating topography of 100-200 meters (Xiao et al. 2003). The climate is mild and humid (sub-tropical continental monsoon climate), with an average temperature of 14 □, and an annual precipitation of 1300~1500 mm (Xiao et al. 2003). There is a surface river running through the study area from north to south. The river bed sediments are thick (~ 1m). In the closed watershed of the study area, river sediments are often dredged out by local residents for cultivation to improve soil fertility. The dredging of the sediment, maintains water drainage but provides a secondary source of material to surface soils.

The morphology of Tl minerals in the study area was dominated by sulfides and sulfosalts of Tl, and the natural mineralization and mining of Tl deposits accelerated the diffusion of Tl into the environment (Xiao et al. 2004a, 2004b). Thallium also exists in coal, local residents have been mining coal seams manually to meet their fuel supply for domestic heating (Xiao et al. 2007).

2.2 Sample collection, treatment and analysis

Sample collection: In the dry season of march 2018, a total of 10 river sediment samples (S1-S10) and 50 surface soil samples (S11-S60) were collected in the study area with sampling intervals of 180~220 m (see Fig. 1). A 0.2 kg sample of soil (0-20 cm depth) was collected at each sampling site, with another four 0.2 kg soil samples collected at locations 2 meters to the northwest, northeast, southeast and southwest directions from the central point. The 5 subsamples formed a 1.0 kg composite sample. After all the samples are collected, water filtered out where appropriate, gravel, wood chips, shells, weeds and other obvious animal and plant residues were removed, and stored in polyethylene plastic bags and labeled before transport back to the laboratory.. The longitude and latitude coordinates of the sampling sites are recorded by GPS.

Sample treatment and analysis: The samples collected above were dried in ambient air and crushed and passed through 200 mesh stainless steel sieves. Samples (0.1 g) were digested in a beaker with concentrated Nitric acid and diluted prior to filtering (0.45um) and analysed for Tl, As, Cd, Cr, Cu, Zn, Pb by ICP-MS (Finnigan MA T). The detection limits were: Tl: 0.005 ng /g, As: 0.1 ng /g, Cd: 0.05 ng /g, Cr: 0.5 ng /g, Cu: 0.1 ng /g, Pb: 0.01 ng /g, Zn: 0.5 ng /g. Accuracy of analysis is verified by quality assurance and quality control procedures. Duplicates (at every 10th sample), reagent blank and national standard soil sample (GBW07401) were used for quality control during instrument testing. The intraclass correlation coefficient (ICC) should be greater than 0.75. The test results of blank samples were all below the detection limit. The error of all element analysis results was controlled within ±10% at 95% confidence level. These experiments were carried out in the Hunan Provincial Key Laboratory of Shale Gas Resource Exploitation.

2.3 Geoaccumulation index (I_{geo})

I_{geo}, proposed by Müller (1969), is widely used in environmental assessment of the significance of enrichments of individual elements in surface environments. The formula is as follows:

$$I_{geo} = \log_2 \frac{C_n}{1.5 * BE_n} \quad (1)$$

C_n is the measured metal concentration in the sample; BE_n is the average geochemical background value of the measured elements. The background value of metal concentration in soil from Guizhou Province was adopted in this study (CNES 1990). I_{geo} can be divided into 7 levels, Levels of less than 0 to greater than 5 indicate the degree of pollution from practically uncontaminated to extremely contaminated (Table S1).

2.4 Enrichment factor (EF)

The EF of each PTE is calculated to quantify the effect of anthropogenic interference on the degree of pollution (Chester and Stoner 1973; Zhu et al. 2017). The EF definition is as follows：

$$EF = \frac{(C_i / C_R)_{sample}}{(C_i / C_R)_{background}} \quad (2)$$

$(C_i/C_R)_{sample}$ is the ratio of the concentration of the elements studied to the reference elements, $(C_i/C_R)_{background}$ is the ratio of geochemical background concentrations of the elements studied to background value of reference elements. Elements such as Al, Ti, Sc orZr are usually used as reference elements (geochemical properties are stable.). For this study and the Al content in the soils of Guizhou Province was selected as the reference element for this study (CNES 1990). In general, an EF value of about 1 indicates that a given metal may come entirely from the crust or natural weathering process (Rashed 2010). For EF>1.5 it is considered an indicator of specific anthropogenic influence. , The EF values falling in ranges 1.5-3, 3-5, 5-10 and > 10 are considered to indicate mild, moderate, severe, and very severe anthropogenic influence (Table S1) (Islam et al. 2015; Milad et al. 2017).

2.5 Potential ecological risk index (RI)

RI, proposed by Swedish scholar Hakanson (1980), is a relatively rapid, simple and standard method for assessing the potential ecological risk level of PTEs in soils or sediments to the environment (Wu et al. 2018). RI can reflect the potential ecological risk caused by the overall pollution level. The formula is as follows:

$$RI = \sum E_r^i = \sum T_r^i (C_s^i / C_n^i) \quad (3)$$

RI is the sum of potential ecological risk indices of various PTEs. E^i_r is a potential ecological risk factor for individual PTEs. C^i_s (mg/kg) is the PTEs content in sample soil. C^i_n (mg/kg) is the background value of PTEs in Guizhou Province (Table 1). T^i_r is the toxicity response factor of each metal. Liu et al (2017b) calculated the toxicity response coefficient of Tl in potential ecological risk assessment, which was set at 10. The toxic response coefficients of As, Cd, Cr, Cu, Pb and Zn were 10, 30, 2, 5, 5, 1 respectively (Hakanson 1980). The classification standard for RI of PTEs is shown in Table S2.

2.6 Health risk of soil PTEs

The local economy is relatively weak and the residents are subsistence farmers, mainly eating food crops they grow in their own fields, resulting in close contact with the soil disrupted by mining, wastes generated over many centuries and also enhanced by the practice of adding potentially contaminated river sediment to farmland. There are three main pathways for human exposure to PTEs: ingestion, inhalation, and dermal contact with PTE enriched particles (Luo et al. 2012). Based on the health risk assessment model recommended by US Environmental Protection Agency, assessment was undertaken for non-carcinogenic and carcinogenic risks in children and adults for the three exposure pathways identified using soil based PTEs from our study (Tl, As, Cd, Cr, Cu, Pb, Zn) . Formula (4)-(11) is used to estimate non-carcinogenic and carcinogenic risks. The mathematical expression is derived from the USEPA (1997) “Exposure factors handbook”. HQ_{ing}、HQ_{der} and HQ_{inh} is the hazard quotient of non-carcinogenic of ingestion, dermal contact and inhalation, respectively. RfD is a reference dose based on USEPA (2013) for non-carcinogenic risk calculation. C_{soil} is the concentration

of PTEs in soil (mg/kg). ABS (unitless) is the dermal absorption factor of 0.03 for As and 0.1 for Pb, and 0.001 for other elements. GIABS is the fraction of pollutant absorbed in gastrointestinal tract (set at 1 based on USEPA (2016)). The HI is the hazard index, the sum of the non-carcinogenic risks of a certain non-carcinogenic pollutant through ingestion, dermal contact and inhalation. It is acceptable when HI≤1. CR_{ing}、CR_{der} and CR_{inh} is the carcinogenic risk of ingestion, dermal contact and inhalation, respectively. TCR is the total cancer risk of three exposure pathways. The acceptable carcinogenic risk threshold recommended by USEPA is: when the carcinogenic risk is acceptable at $1\times10^{-6}<R<1\times10^{-4}$; the risk of $R<1\times10^{-6}$ can be neglected; when $R>1\times10^{-4}$, it is unacceptable carcinogenic risk, and measures must be taken to reduce the risk. The meanings and values of the other parameters are shown in Tables S3 and S4.

$$HQ_{ing} = \frac{C_{soil} \times IngR \times EF \times ED}{BW \times AT \times RfD_{ing}} \times CF \quad (4)$$

$$HQ_{der} = \frac{C_{soil} \times SA \times AF_{soil} \times ABS \times EF \times ED}{BW \times AT \times RfD_{der}} \times CF \times GIABS \quad (5)$$

$$HQ_{inh} = \frac{C_{soil} \times InhR \times EF \times ED}{PEF \times BW \times AT \times RfD_{inh}} \quad (6)$$

$$HI = \Sigma HQ = HQ_{ing} + HQ_{inh} + HQ_{der} \quad (7)$$

$$CR_{ing} = \frac{C_{soil} \times IngR \times EF \times ED}{BW \times AT} \times CF \times SF_{ing} \quad (8)$$

$$CR_{der} = \frac{C_{soil} \times SA \times AF_{soil} \times ABS \times EF \times ED}{BW \times AT} \times CF \times SF_{der} \quad (9)$$

$$CR_{inh} = \frac{C_{soil} \times InhR \times EF \times ED}{PEF \times BW \times AT} \times SF_{inh} \quad (10)$$

$$TCR = CR_{ing} + CR_{inh} + CR_{der} \quad (11)$$

2.7 Statistical methods

Pearson correlation coefficient matrix (Table 2), principal component analysis (PCA) and rotational component matrix (Table 3) were obtained from 60 samples of 7 PTEs in soil by SPSS (IBM, USA) software. Pearson correlation analysis is used to find out the correlation between various elements, which provides effective information for explaining the sources of PTEs in the environment (Manta et al. 2002). Principal component analysis (PCA) is an effective method to identify and explore the pollution sources of PTEs in the environment (Wang et al. 2015). In ArcGIS 10.3 (ESRI, Redlands, California, USA), the spatial distribution map of PTEs concentration, degree of pollution and ecological risk in the study area is visually displayed in graphical form.

3. Results and discussions

3.1 Spatial distribution of PTEs

The average concentrations of Tl, As, Cd, Cr, Cu, Pb and Zn were 28.82 mg/kg, 133.75 mg/kg, 1.14 mg/kg, 52.11 mg/kg, 79.63 mg/kg, 44.39 mg/kg and 118.23 mg/kg, respectively (see Table 1) and were 40.48, 6.69, 1.73, 0.54, 2.49, 1.26, and 1.19 times the background values of soil in Guizhou Province, respectively. The coefficients of variation (CV) of Tl, As, Cd, Cr, Cu, Pb and Zn were 75%, 76%, 116%, 47%, 32%, 48% and 58% respectively. The high variability suggesting discrete inputs related to natural or external factors (Zhao et al. 2010). The high average concentration, extreme

maximum and high variability of Tl and As (and to an extent Cd) indicate that their spatial distribution may be mainly disrupted by inputs from human activities, such as mining, industrial enterprises and other production activities (Li et al. 2017). The concentration of Cd in the sampling sites (S1-S10) of surface sediments of rivers is extremely high compared with that in soil samples, which is the reason for high spatial variability of Cd. Yuan et al. (2018) also reported that river sediments are heavy metal-rich sites. The moderate variability and concentration of Cu, Pb and Zn suggest that they have been locally contaminated in the study area. Kriging interpolation is performed on the Tl, As, Cd, Cu, Pb, Zn sample data on ArcGIS10.3 (ESRI, Redlands, California, USA) (Fig. 2) to obtain visual information about the spatial distribution of PTEs. The low variability of Cr and its maximum concentration close to the background value, indicating that Cr has little anthropogenic disturbance, is free of contamination in the study area, and was not used in the ArcGIS visualization..

The highest concentrations of Tl and As are found on mining slopes with higher terrain in the central part of the area (Fig. 2), close to main mining locations. The Cd, Pb and Zn are enriched in the West,which is consistent with the spatial location of river and road. The distribution of Cu is slightly higher in the north and south of the region. According to the spatial distribution of PTEs and on-site investigation in the study area, the following three points are obtained:

In the first, coal mining is the most direct introduction of PTEs into the surface environment (Hua rt al. 2018). The high inputs of Tl, As and its residues are concentrated in coal mines, clay mines, and other wastes in the central zone of the study area, that can migrate downhill, onto farmland and into surface waters. These wastes are also often used by local residents to increase the height of riverbanks. This is the main reason why the Tl and As are enriched in the river sediments . Leaching or weathering of cinders and gangues can also provide thallium downhill to the soils, rivers, and can be enriched in river sediment. In addition, under flood conditions, sediments are easily mixed with water, and PTE -rich sediments are enriched in the soil around the river and in the lower lying terrain (Yuan et al. 2018). It can be seen that river sediments are not only the enrichment area of PTEs pollutants, but also the secondary pollution sources with potential hazards to water quality and the surrounding environment.

Secondly, the distribution of thallium and other PTEs in soil may also be disturbed by agricultural activities. Agricultural activities include transporting the soil from upstream to downstream or down slope by local farmers to improve soil fertility. These soils tend to contain slag or coal ash fragments, which is important evidence of anthropogenic influence. In addition, some abandoned coal mines have been locally exploited by residents, and cinders were used to fill roads or add to arable land.

Thirdly, the leaching of rainwater through surface cracks can enhance migration of the PTEs forming secondary minerals on the surface of cracks or rocks by evaporating after rainwater leaching (Hua et al. 2018; Yang et al. 2018). Over many centuries, the dual effects of leaching and evaporation have led to the release of thallium sulfate into the surrounding ecosystem (Xiao et al. 2004a, 2004b). High rainfall in the area enhancing this process.

3.2 PTE pollution and source contributions

The order of decreasing average I_{geo} for soil PTEs in the study area is: Tl > As > Cu > Pb > Cd > Zn > Cr. With the average I_{geo} for Tl and As of 4.28 and 1.69 respectively, it is clear that for Tl the areas is heavily to extremely contaminated, and for As a level of moderate pollution has been reached. At the hillside locations with higher topography, the pollution level of Tl and As was the greatest (Fig. S1), reducing progressively down slope. The average I_{geo} value of Cu is 0.66. Illustrated in Fig. S1, the distribution of Cu in the study area shows uncontaminated to moderately contaminated levels across the location, evenly distributed. The average I_{geo} values of other elements are less than 0, indicating that

for Cd, Cr, Pb and Zn the area is relatively uncontaminated.

The enrichment factors of PTEs at all sampling sites (Fig. S2) and their average values (Table 1) show Tl distribution is seriously affected by anthropogenic influence (EF>10), especially in the upstream rivers, mining sites and down slope farmland near the mining areas (Fig. S2). Pollution by As pollution shows serious anthropogenic influence (5 <EF≤10), and the enrichment sites was similar to that of Tl. Cu was slightly affected by anthropogenic activity (1.5 <EF≤3) but enriched uniformly throughout the study area. Cr and Pb may be derived from crustal matter or natural weathering process (EF ≤1.5). The significant input to Cd levels was in river sediments (5<EF≤10), with Zn was slightly enriched in sampling sites around roads (1.5<EF≤3), Cd and Zn were not identified to be affected by human activities at other sites (EF≤1.5).

A number of multivariate statistical assessments (e.g. correlation coefficient matrix, principal component analysis and rotating component matrix) have previously been successfully used to identify discrete inputs of PTEs n surface soils (Acosta et al . 2011; Manta et al. 2002). A strong correlation was found between several element pairs (r^2 > 0.5) (Table 2). The correlation between Tl and As was the best (r^2 = 0.798), followed by Cd and Zn (r^2 = 0.748), Cr and Cu (r^2 = 0.614). Lower correlation was found between Pb and other elements. The high correlation between PTEs suggests that they may have a common source, or have similar behavior in the transformation, or have similar transport pathways under the physical and chemical conditions prevailing at the site (Li et al. 2017; Wang et al. 2012).

Through principal component analysis (Table 3), three principal components with eigenvalues greater than 1.0 were obtained, which explained nearly 80% of the data variability. According to the rotating component matrix (Table 3), the PTE groupings indicate associations with the first principal component (PC1) contributes 39.1% of the cumulative variance, in which Tl and As loads are very high and other elements loads are low, and there is a strong correlation between Tl and As (Table 2), suggesting Tl and As share one or more common sources. The field investigations corroborate this with mining wastes rich in thallium and arsenic exposed on the ground and hillside as the direct source of Tl and As pollution. These mine wastes are located on the high-altitude parts of the study area, and transferred to surrounding and downhill soils and rivers through physical transport is likely (Hua et al.2018; Yang et al. 2018), which is consistent with the spatial distribution maps for Tl and As. Many previous studies have shown that As is a product of coal-fire emissions from materials mined in the region (Guo et al. 2006; Xie et al. 2006; Yang et al. 2003; Zhang et al. 2018). Therefore strong inputs from local Tl and As coal mining and combustion contributes to the dispersal of Tl and As. This is supported by the EF data presented previously. Typical activities such as mining operations, tailings, waste water, and atmospheric emission contribute to the dominance of the first principal component.

The second principal component contributed just over 25% of the total variance with high loads from Cd and Zn. The data in Table 2 show strong correlation between Cd and Zn. Direct sources may be difficult to confirm as e.g. tire tread (Fauser et al. 1999) and dust from tire friction (Adachi and Tainoshob. 2004; Apeagyei et al. 2011; Schauer et al. 2006) can be enriched in Zn, and the traffic infrastructure shows an important traffic route across the study area and high vehicle traffic. Therefore, the main source of Zn in the study area can be tire wear of freight cars and other transport vehicles. Milad et al. (2018) came to a similar conclusion in studies of the spatial distribution of heavy metals in road dust in Rafsanjan, SE Iran. According to field investigation (agricultural and topographical features), agricultural supplies such as pesticides, fertilizers and other agricultural products widely used in the region contain high levels of Cd, partly absorbed by crops, partly because rain water flows into rivers and accumulates in river sediments all the year round (Yuan et al. 2018). Cai et al. (2012) has

reported this in studies of heavy metals in farmland soil. It has also been shown that Cd exists mainly in chemical fertilizers and is a marker element of agronomic practices (Milad et al. 2018). The road is not only adjacent to the river, but also runs through the study area from north to south. It was found that the content of Cd in the first ten sample data (river surface sediments) was abnormally high, which may be the reason for the high correlation between Cd and Zn. In addition, phosphorus fertilizers and chemical pesticides also contain Zn and Cd (Charlesworth et al. 2011) , which may also contribute to similar spatial distributions of Zn and Cd. The spatial distribution discussed in section 3.1 adds further support to this indicative source apportionment.

The third principal component contributed approximately 15% of the cumulative variance, with contributions from Cr, Cu, and Pb . According to Table 2, the correlation between Cr and Cu is high, and the correlation between Cr and Pb is modest, with Cu and Pb not being strongly correlated, indicating that Cu and Pb have different sources. The enrichment factor of Pb is 1.21, slightly less than 1.5, and the spatial distribution of Pb shows that Pb is enriched along the road (Fig. 2), so it is arbitrary to attribute Pb to natural sources discussed above. Pb is a component of automobile exhaust (gasoline) (Carolina et al. 2018; Liang et al. 2017; Wang et al. 2018), and the spatial distribution map of Pb concentration is consistent with this view. It has been inferred from the enrichment factor that Cr is a natural source (EF=0.52), while Cu is only slightly affected by anthropogenic activities ($1.5 < EF \leq 3.0$), indicating that there are other sources of Cu in PC3. The contribution to Cu may be a mixture of combustion of coal, oil and refuse (Yang et al. 2002). It is known from field investigation that coal mining has been carried out for hundreds of years in the study area, and the ash from coal combustion is often used by local residents to pave rural roads or as additives for garden soil. The copper-containing waste gas and slag produced by coal combustion are the sources of copper pollution.

3.3 Ecological risks assessment

The average potential ecological risk (E_r^i) of single metals are: Tl (404.75)> As (66.87)> Cd (51.94)> Cu (12.44)> Pb (6.31)> Zn (1.19)> Cr (1.09). Tl has reached a very high level of ecological risk, As and Cd are at a moderate level of risk, and other metals are in the low ecological risk range (Fig. 3). Spatial visualization of RI for all seven PTEs and the E_r^i for Tl, As, Cd is shown in Figure 3. The range of RI in the study area is 91.25.13-1479.34 Approximately 10% of sampling sites are at considerable ecological risk and just over 23% of sampling sites are at high ecological risk with around 66% of sampling sites are at very high ecological risk. The contribution Tl to the total RI is 74.32% and that of As and Cd to RI is 8.57% and 7.32%, respectively with the total contribution of Cu, Pb, Zn and Cr to RI is only around 4%. Besides, the ecological risk of Tl at different sampling points is in good agreement with the RI of corresponding sampling sites. The ecological risk of Tl in soil of this area needs to be should be paid more attention to. From Figure 3 it can be seen that the RI is the highest around the mining sites with high topography, and gradually decreasing along the downhill, which also indicates that Tl and As in the study area mainly come from mining activities.

Compared with other studies, thallium has never been considered in soil ecological risk assessment in other regions, whilst Cd poses the highest potential ecological risk in many study areas (Apeagyei et al. 2011; Feng et al. 2018; Lin et al. 2019; Shen et al. 2017; Zhang et al. 2018). A number of PTEs have been identified often associated with local environmental drivers e.g. As in the study of Yuan et al. (2018); Sb in a mining region (Fei et al. 2017) and Cd with Hg in a typical county of Shanxi Province, China (Pan et al. 2016). Consequently the results of our assessment add considerably to the relatively poor international perspective on the environmental impact of Tl..

3.4 Health risk assessment

Health risk analysis of PTEs contamination in soil sampling sites (S11-S60) was conducted to obtain non-carcinogenic risks (Table S5, Fig. 4) and carcinogenic risks (Table S6, Fig. 4) for adults and children under different exposure pathways. The order of non-carcinogenic risk of PTEs to adults and children is As > Tl > Pb > Cr > Cu > Cd > Zn (Table S5). For adults, the HI values of Tl, As, Cd, Cr, Cu, Pb and Zn is less than 1, indicating that they are not at non-carcinogenic risk (Table S5). The total HI value of all PTEs was 1.66 for adults, which is greater than the threshold of 1.0, and the contribution of Tl and As were 35.66% and 57.89% respectively. The non-carcinogenic risk indices of Tl and As were 4.69 and 7.15, respectively. Cd, Cr, Cu, Pb and Zn had no non-carcinogenic risk for children (HI ＜1). The total HI value of all PTEs was 12.6 for children, and the contribution for Tl and As were 37.22% and 59.60% respectively. Figure 4a and 4b shows that the non-carcinogenic risk of children under different exposure pathways is significantly higher than that of adults, and the hazard quotient of children is 7.6 times than that of adults, indicating that children are more vulnerable to PTEs in the soil than adults. The order of non-carcinogenic hazards under ingestion, dermal contact and inhalation was: HQ_{ing} > HQ_{der} > HQ_{inh} (Fig. 4a, 4b). Adults and children's ingestion of PTEs accounted for 82.5% and 86.5% of the non-cancer risk, respectively, and dermal contact for PTEs accounted for 17.5% and 13.1% of the non-cancer risk, respectively. The risk of dermal contact is usually more than 100 times the risk of inhalation. Ingestion of Tl and As were the major contributors to non-cancer risk, with 79.3% and 83.5% of adults and children, respectively. Dermal contact with As was a secondary factor for non-carcinogenicity risk, with 13.1% in adults and 9.7% in children, respectively. Among the elements studied, As is the major non-carcinogenic element in the three pathways of ingestion, dermal contact and inhalation.

The total carcinogenic risk of As, Cd, Cr and Pb to adults and children was 1.48×10^{-4} and 2.76×10^{-4} (Table S6), respectively. It indicates that children are more vulnerable to the carcinogenic effects of PTEs in soil. The carcinogenic risk of adults and children is higher than the level of 1.0×10^{-4}, which is an unacceptable carcinogenic risk, and almost all of the risks come from As. The order of carcinogenic risks under ingestion, dermal contact and inhalation was: CRing＞CRder＞CRinh (Fig. 4c, 4d). Ingestion of As was the main role of leading to carcinogenic, accounting for 77.0% and 83.0% of the total carcinogenic risk in adults and children, respectively, while dermal contact accounted for 22.6% and 17.0%, respectively. Inhalation of PTEs had low significance in this study.

4. Conclusion

Source identification of PTEs helps to define areas of priority control, and the assessment of ecological-health risks is important to identify the relative contribution of specific elements in specific regions compared to ecological and health hazards. This helps to properly prioritize the control and management of PTEs in the environment.

(1) Tl pollution shows serious contamination levels along with As and to a lower degree Cu. Other elements are almost uncontaminated in the study area as a whole. Tl poses the highest potential ecological risk. The risk of human health caused by PTEs in soil is mainly caused by oral ingestion, dermal contact and inhalation have little effect. The main hazards to human health are As and Tl (especially for children), and other elements have a negligible risk for the health of residents in the study area.

(2) The contamination distribution patterns of PTEs correspond to the mining sites as well as along the river and roads. These distribution patterns are related to a number of discrete primary and secondary pollution sources, such as mining, traffic, coal burning, agricultural pollution.

Different sources contribute to ecological and human health risk to varying degrees. Mining activities and waste erosion are the main reasons for the high risks of ecological-health in the study area. Tl is dominant but secondary sources around road and river features have also been identified to be of concern in the study area.

(3) Management of the soil contamination requires different approaches – the primary processing residues from mining need to be stabilized and isolated. Agricultural inputs through secondary use of contaminated material needs to be reversed. Contaminated farmland needs to be stabilized-used for other (non food) or low-enriched PTEs crops to prevent further transfer in the food chain.

Acknowledgments

This work was supported by the National Natural Science Foundation of China (NO. 41472328).

References

Acosta JA, Gabarrón M, Faz, A et al (2015) Influence of population density on the concentration and speciation of metals in the soil and street dust from urban areas. Chemosphere 134: 328-337

Adachi K, Tainosho Y (2004) Characterization of heavy metal particles embedded in tire dust. Environ Int 30: 1009-1017

Anagboso MU, Turner A, Braungardt C (2013) Fractionation of thallium in the Tamar estuary, South West England. J Geochem Explor 125: 1-7

Apeagyei E, Bank MS., Spengler JD et al (2011) Distribution of heavy metals in road dust along an urban-rural gradient in Massachusetts. Atmos Environ 45: 2310-2323

Azhari AE, Rhoujjati A, Hachimi MLE et al (2017) Pollution and ecological risk assessment of heavy metals in the soil-plant system and the sediment-water column around a former Pb/Zn-mining area in NE Morocco. Ecotox Environ Safe 144: 464-474

Cai L, Xu Z, Ren M et al (2012) Source identification of eight hazardous heavy metals in agricultural soils of Huizhou, Guangdong Province, China. Ecotox Environ Safe 78: 2-8

Carolina R, Emma L.T, Walter G et al (2018) Trace element and Pb isotope fingerprinting of atmospheric pollution sources: A case study from the east coast of Ireland. Appl Geochem 96: 302-326

CEMS (1990) Chinese Environmental Monitoring Station. Soil Background Values of China; Chinese Environmental Science Press: Beijing, China. (In Chinese)

Charlesworth S, De Miguel E, Ordóñez A (2011) A review of the distribution of particulate trace elements in urban terrestrial environments and its application to considerations of risk. Environ Geochem Health 33: 103–123

Chen Y, Jiang X, Wang Y et al (2018) Spatial characteristics of heavy metal pollution and the potential ecological risk of a typical mining area: a case study in china. Process Saf Environ 113: 204-219.

Chen Y, Xie W, Wu Y et al (2001) Utilization of Mineral Resources Containing Thallium and Thallium Pollution in China. Journal of Shenzhen University: science and Technology 18: 57-63. (In Chinese)

Chester R, Stoner J.H, 1973. Pb in particulates from the lower atmosphere of the eastern Atlantic. Nature 245: 27-28

Fauser P, Tjell JC, Mosbaek H et al (1999) Quantification of tire-tread particles using extractable organic zinc as tracer. Rubber Chem Technol 72: 969-977

Fei JC, Min XB, Wang ZX et al (2017) Health and ecological risk assessment of heavy metals pollution in an antimony mining region: a case study from South China. Environ Sci Pollut Res (2017) 24: 27573-27586

Feng J, Bozhi R, Hursthouse A.S. et al (2018) Trace Metal Pollution in Topsoil Surrounding the Xiangtan Manganese Mine Area (South-Central China): Source Identification, Spatial Distribution and Assessment of Potential Ecological Risks. Int J Env Res Pub He 15: 2412

Guo X, Gao R, Huang R et al (2006) Study on the characteristics of inorganic elements in atmospheric particulate matter. Environmental science and technology, 29: 49-51 (In Chinese)

Hakanson L (1980) An ecological risk index for aquatic pollution control: a sedimentological approach. Water Res 14: 975-1001

Hua C, Zhou G, Yin X et al (2018) Assessment of heavy metal in coal gangue: distribution, leaching characteristic and potential ecological risk. Environ Sci Pollut Res 25:32321-32331

Islam MS, Ahmed MK, Raknuzzaman M et al (2015) Heavy metal pollution in surface water and sediment: a preliminary assessment of an urban river in a developing country. Ecol Indic 48: 282-291

Jia Y, Xiao T, Zhou G et al (2013) Thallium at the interface of soil and green cabbage (Brassica oleracea L. var. capitata L.): soil-plant transfer and influencing factors. Sci Total Environ 450-451: 140-147

Kaplan DI, Mattigod SV (1998) Aqueous geochemistry of thallium. In:Nriagu, J.O.(eds.),Thallium in the Environment. John Wiley& Sons, Inc, New York 15-29

Karakus PBK (2012) Determination of heavy metals in indoor dust from Istanbul, Turkey: estimation of the health risk. Environ Int 50: 47-55

Rashed MN (2010) Monitoring of contaminated toxic and heavy metals, from mine tailings through age accumulation, in soil and some wild plants at Southeast Egypt. J Hazard Mater 178: 739–746

Lin W, Wu K, Lao Z et al (2019) Assessment of trace metal contamination and ecological risk in the forest ecosystem of dexing mining area in northeast Jiangxi province, china. Ecotox Environ Safe 167: 76-82

Li X, Yang H, Zhang C et al (2017) Spatial distribution and transport characteristics of heavy metals around an antimony mine area in central China. Chemosphere 170: 17-24

Liang J, Feng C, Zeng G et al (2017) Spatial distribution and source identification of heavy metals in surface soils in a typical coal mine city, Lianyuan, China. Environ Pollut 225: 681-690

Liu J, Luo X, Jin W et al (2017a) Thallium contamination in arable soils and vegetables around a steel plant - a newly-found significant source of tl pollution in south china☆. Environ Pollut 224: 445-453

Liu Y, Wang Q, Zhuang W et al (2017b) Calculation of thallium's toxicity coefficient in the evaluation of potential ecological risk index: a case study. Chemosphere 194: 562-569

Luo XS, Ding J, Xu B et al (2012) Incorporating bioaccessibility into human risk assessments of heavy metals in urban park soils. Sci Total Environ 424: 88-96

Manta DS, Angelone M, Bellanca A et al (2002) Heavy metals in urban soils: a case study from the city of Palermo (Sicily), Italy. Sci Total Environ 300: 229-243

Mcgrath SP, Lane PW (1989) An explanation for the apparent losses of metals in a long-term field experiment with sewage sludge. Environ Pollut 60: 235-256

Milad MA, Mohammed B, Rouhollah M et al (2017). The ecological risk, source identification, and pollution assessment of heavy metals in road dust: a case study in Rafsanjan, SE Iran. Environ Sci

Pollut Res 4: 13382–13395

Pan L, Ma J, Hu Y et al (2016) Assessments of levels, potential ecological risk, and human health risk of heavy metals in the soils from a typical county in Shanxi Province, China. Environ Sci Pollut Res 23: 19330-19340

Pareja-Carrera J, Mateo R, Rodriguez-Estival J (2014) Lead (Pb) in sheep exposed to mining pollution: implications for animal and human health. Ecotox Environ Safe 108: 210-216

Pascaud G, Leveque T, Soubrand M et al (2014) Environmentaland health risk assessment of Pb, Zn, As and Sb in soccer field soils and sedimentsfrom mine tailings: solid speciation and bioaccessibility. Environ Sci Pollut R 21: 4254-4264

Peter ALJ, Viraraghavan T (2005) Thallium: a review of public health and environmental concerns. Environ Int 31: 493-501

Sani HA, Ahmad MB, Hussein MZ et al (2017) Nanocomposite of ZnO with montmorillonite for removal of lead and copper ions from aqueous solutions. Process Saf Environ 109: 97-105

Schauer JJ, Lough GC, Shafer MM et al (2006) Characterization of metals emitted from motor vehicles. Research Report 133: pp 1

Siegel BZ, Siegel SM (1976). Thallium antagonism toward potassium dependent systems. Bioinorg. Chem Appl 6: 229-232.

Stewart A, Hursthouse A (2018) Environment and human health: the challenge of uncertainty in risk assessment. Geosciences 8: pp 24

Sun Y, Zhou Q, Xie X et al (2010) Spatial, sources and risk assessment of heavy metal contamination of urban soils in typical regions of Shenyang, China. J Hazard Mater 174: 455-462

USEPA (1997) Exposure factors handbook. EPA/600/P-95/002F. DC: Environmental Protection Agency, Office of Research and Development, Washington,

USEPA (2013) Region IX, regional screening levels (formerly PRGs). San Francisco, CA 94105. Available at: http://www.epa.gov/region9/superfund/prg/

USEPA (2016) Regional Screening Levels (RSLs) - User's Guide available on. https://www.epa.gov/risk/regionalscreening-levels-rsls-users-guide-may-2016.

Wang C, Chen Y (2007) Thallium in the environment and its health effects. Journal of Guangzhou University (Natural Science Edition) 6: 50-54. (In Chinese)

Wang S, Cai LM, Wen HH et al (2018) Spatial distribution and source apportionment of heavy metals in soil from a typical county-level city of Guangdong Province, China. Sci Total Environ 655: 92-101

Wang Y, Yang L, Kong L et al (2015) Spatial distribution, ecological risk assessment and source identification for heavy metals in surface sediments from Dongping lake, Shandong, East China. Catena 125: 200-205

Wang Y, Hu J, Xiong K et al (2012) Distribution of heavy metals in core sediments from Baihua Lake. Procedia Environmental Sciences. 16: 51-58

Wappelhorst O, Kühn I, Oehlmann J et al (2000) Deposition and disease: amoss monitoring project as an approach to ascertaining potential connections. Sci Total Environ 249: 243-256

Wu W, Wu P, Yang F et al (2018) Assessment of heavy metal pollution and human health risks in urban soils around an electronics manufacturing facility. Sci Total Environ 630: 53-61

Xiao T, Dan B, Guha J et al (2003) Groundwater-related thallium transfer processes and their impacts on the ecosystem: southwest Guizhou province, China. Appl Geochem 18: 675-691

Xiao T, Guha J, Dan B et al (2004a) Naturally occurring thallium: a hidden geoenvironmental health

hazard? Environ Int 30: 501-507

Xiao T, Guha J, Boyle D et al (2004b) Environmental concerns related to high thallium levels in soils and thallium uptake by plants in southwest Guizhou, China. Sci Total Environ 318: 223-244

Xiao T, Guha J, Liu, C.Q et al (2007) Potential health risk in areas of high natural concentrations of thallium and importance of urine screening. Appl Geochem 22: 919-929

Xiao T, Yang F, Li S et al (2012) Thallium pollution in china: a geo-environmental perspective. Sci Total Environ 421-422: 51-58

Xie R, Seip HM, Wibetoe G et al (2006) Heavy coal combustion as the dominant source of particulate pollution in taiyuan, china, corroborated by high concentrations of arsenic and selenium in PM10. Sci Total Environ 370: 409-415

Yang F, He K, Ma Y et al (2003) Characteristics and sources of microelement concentration change in Beijing atmospheric PM2.5. Environmental Science. 24: 33-37 (In Chinese)

Yang L, Chen F (2002) Study on sources of atmospheric dust pollutants in Lanzhou. Journal of Environmental Science. 22: 499-502 (In Chinese)

Yang R, Li Z, Huang B et al (2018) Effects of Fe(III)-fulvic acid on Cu removal via adsorption versus co-precipitation. Chemosphere 197:291-298

Yuan H, Song S, An, S et al (2018) Ecological risk assessment of potentially toxic elements (PTEs) in the soil-plant system after reclamation of dredged sediment. Environ Sci Pollut Res 25: 29181-29191

Zhang P, Qin C, Hong X et al (2018) Risk assessment and source analysis of soil heavy metal pollution from lower reaches of Yellow River irrigation in China. Sci Total Environ 633: 1136-1147

Zhang W, Sun Q, Yang X (2018) Thermal effects on arsenic emissions during coal combustion process. Sci Total Environ 612: 582-589

Zhao K, Liu X, Xu J et al (2010) Heavy metal contaminations in a soil-rice system: identification of spatial dependence in relation to soil properties of paddy fields. J Hazard Mater 181: 778-787

Zhu L, Liu J, Xu S et al (2017) Deposition behavior, risk assessment and source identification of heavy metals in reservoir sediments of Northeast China. Ecotox Environ Safe 142: 454-463

Zitko V (1975) Toxicity and pollution potential of thallium. Sci Total Environ 4: 185-192

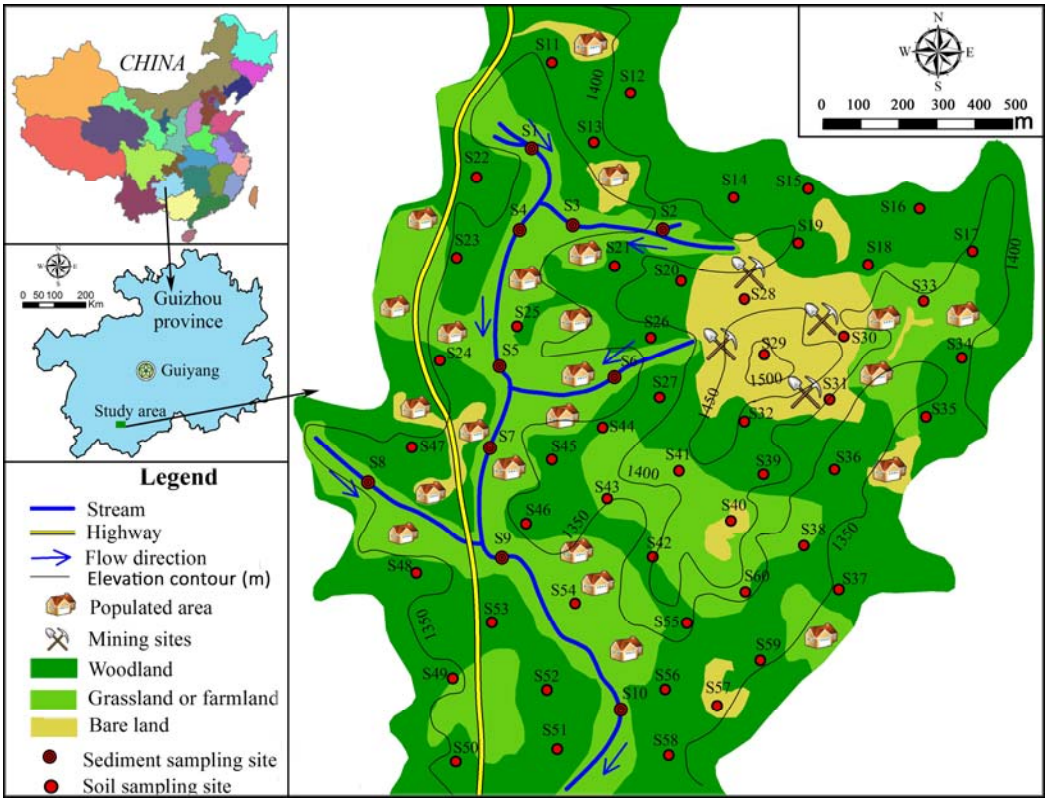

Fig. 1. Simplified map of the study area and sampling locations.

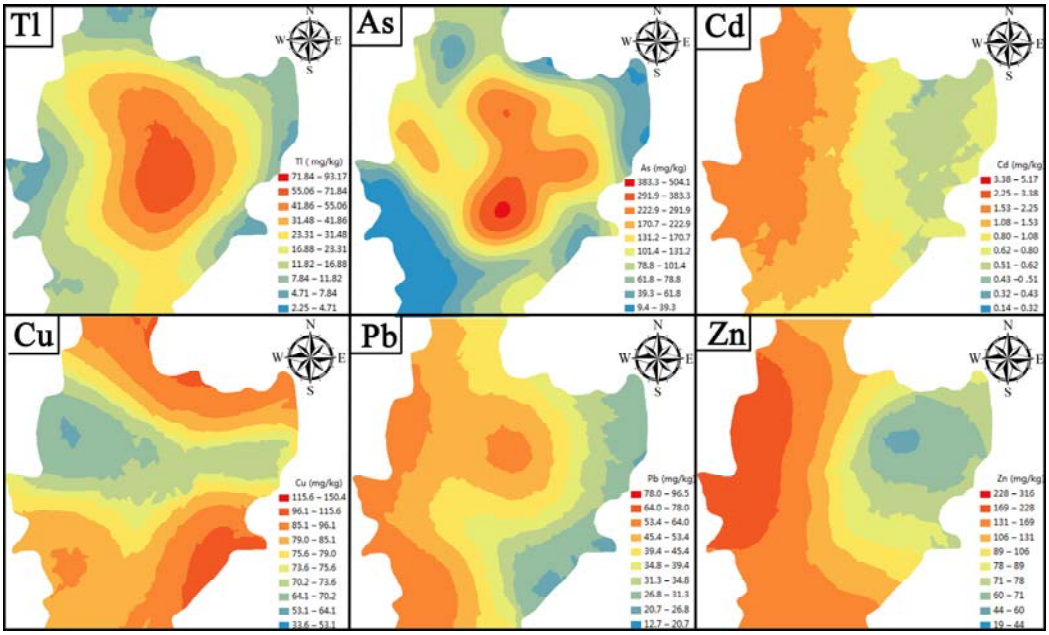

Fig. 2. Concentration distribution maps of PTEs (Tl、As、Cd、Cu、Pb、Zn) in soil over the study area.

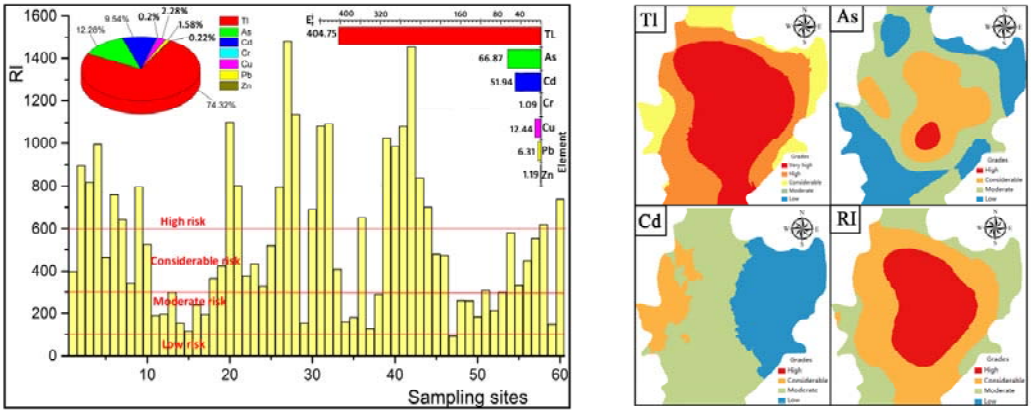

Fig.3.E_r^i scatter of PTEs and RI diagram of samples (As the left). Maps of interpolated potential ecological risk index values for the study area (As the right).

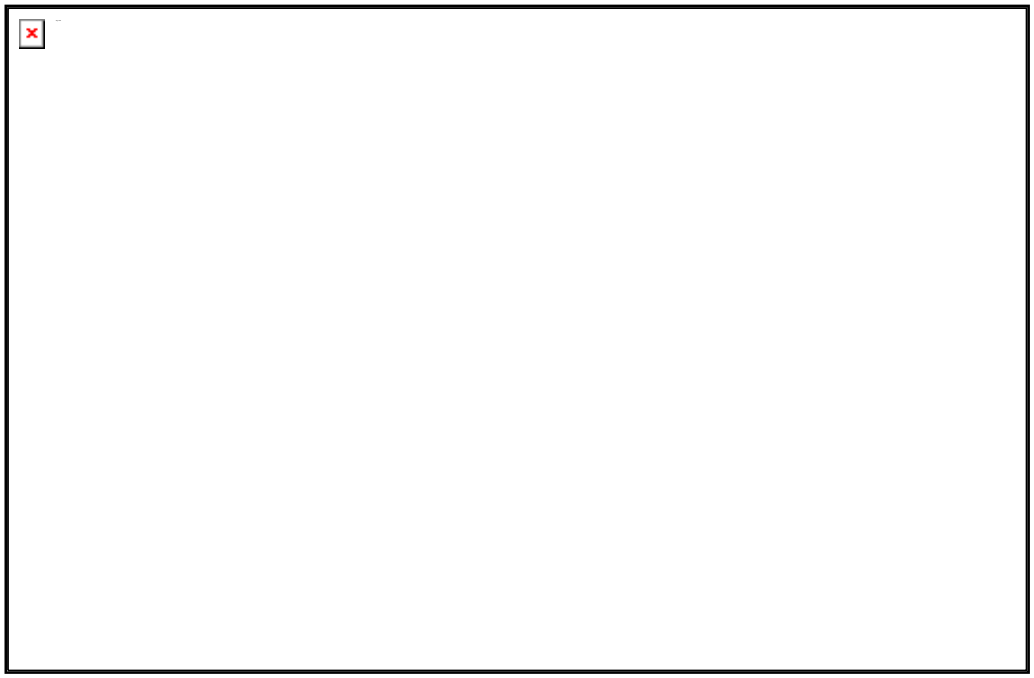

Fig. 4. Non-carcinogenic risks of soil PTEs in the sampling sites: (a)Adults; (b)Children. Carcinogenic risks of soil PTEs in the sampling sites: (c)Adults; (d)Children.

Table 1 Descriptive statistics for PTEs concentration and basic parameters in soils (mg/kg).

Element	Min	Max	Mean±S.D	CV(%)	B V	EF	I_{geo}
Tl	2.25	93.17	28.82±21.65	75	0.712	38.86	4.28
As	9.43	504.10	133.75±101.08	76	20.0	6.42	1.69
Cd	0.14	5.17	1.14±1.32	116	0.659	1.66	-0.42
Cr	8.69	108.83	52.11±24.59	47	95.9	0.52	-1.64
Cu	33.62	150.45	79.63±25.18	32	32	2.39	0.66
Pb	12.73	96.46	44.39±21.42	48	35.2	1.21	-0.41
Zn	18.51	316.40	118.23±68.90	58	99.5	1.14	-0.57

Min = minimum; Max = maximum; CV = coefficient of variation; S.D = standard deviation.

BV=Background Values, According to the Background value of soil elements in China (China National Environmental Monitoring Centre, 1990)

EF and Igeo are the mean values of enrichment factor and geological accumulation index for PTEs in the study area.

Table 2 Pearson correlation coefficients for PTEs in soil.

	Tl	As	Cd	Cr	Cu	Pb	Zn
Tl	1						
As	**0.798****	1					
Cd	0.002	-0.131	1				
Cr	-0.394**	-0.478**	0.296*	1			
Cu	-0.303*	-0.324*	-0.096	**0.614****	1		
Pb	0.212	0.166	0.053	-0.412**	-0.202	1	
Zn	-0.172	-0.287*	**0.748****	0.292*	-0.033	0.231	1

** Indicates that correlation is significant to a level of 0.01(2-tailed).

* Indicates that correlation is significant to a level of 0.05 (2-tailed).

Table 3 Total variance and principal component analysis for PTEs concentration in soils .

Component	Initial eigenvalues			Element	Rotated Component		
	Total	% of variance	Cumulative %		PC1	PC2	PC3
1	2.737	39.1	39.1	Tl	**0.925**	0.000	-0.174
2	1.806	25.8	64.9	As	**0.907**	-0.160	-0.199
3	1.047	15.0	79.9	Cd	0.056	**0.937**	0.042
4	0.805	11.5	91.4	Cr	-0.305	0.360	**0.801**
5	0.223	3.2	94.6	Cu	-0.283	-0.059	**0.702**
6	0.205	2.9	97.5	Pb	-0.015	0.173	**-0.756**
7	0.177	2.5	100.0	Zn	-0.213	**0.913**	-0.109

PC1: The first principal component.

PC2: The second principal component.

PC3: The third principal component.

Supplementary Materials

Distribution, source identification, and ecological-health risks of potentially toxic elements (PTEs) in soil of thallium mine area (Southwestern Guizhou, China)

Feng Jiang [a, b], Bozhi Ren[*a, b], Andrew Hursthouse[a, c], Renjian Deng [a, b], Zhenghua Wang [a]

Table S1 Grades of Igeo and EF (see Islam, 2015).

Table S2 Indices and grades of potential ecological risk (Hakanson, 1980).

Table S3 Exposure factors used in estimation for non-carcinogenic risk.

Table S4 References dose (RfD) for non-carcinogenic metals and slope factor (SF) for carcinogenic metals.

Table S5 Hazard quotient (HQ) and cumulative hazard index (HI) for non-carcinogenic risk.

Table S6 Carcinogenic risk of adults and children under different exposure pathways.

Fig. S1. Geoaccumulation index (I_{geo}) maps of Tl, As and Cu in soil over the study area.

Fig. S2. Enrichment factor of PTEs in river sediment (S1-S10) and topsoil (S11-S60).

Table S1 Grades of Igeo and EF (see Islam, 2015).

I_{geo}	Pollution level	EF	Influence sources
$I_{geo}\leq 0$	Practically uncontaminated	EF≤1.5	entirely from natural
$0<I_{geo}\leq 1$	Uncontaminated to moderately contaminated	1.5＜EF≤3	Minor Anthropogenic influence
$1<I_{geo}\leq 2$	Moderately contaminated	3＜EF≤5	Moderate Anthropogenic influence
$2<I_{geo}\leq 3$	Moderately to heavily contaminated	5＜EF≤10	Severe Anthropogenic influence
$3<I_{geo}\leq 4$	Heavily contaminated	10＜EF	Very severe Anthropogenic influence
$4<I_{geo}\leq 5$	Heavily to extremely contaminated		
$I_{geo}>5$	Extremely contaminated		

Table S2 Indices and grades of potential ecological risk (Hakanson, 1980).

Index	Grades of ecological risk pollution				
	Low risk	Moderate risk	Considerable risk	High risk	Very high risk
E^i_r	$E^i_r<40$	$40\leq E^i_r<80$	$80\leq E^i_r<160$	$160\leq E^i_r<320$	$E^i_r\geq 320$
RI	RI＜150	150≤RI＜300	300≤RI＜600	RI≥600	

Table S3 Exposure factors used in estimation for non-carcinogenic risk.

Variables	Value
IngR (mg/day): Soil ingestion rate	100 (adult); 200 (children)
EF (days/year): Exposure frequency	350 days
ED (years): Exposure duration	24 (adult); 6 (children)
BW (kg): Average body weight	60 (adult); 15 (children)
AT (days): Averaging time	365×ED adult/children(non-carcinogenic); 365×70 (carcinogenic risk)
CF (kg/mg): Conversion factor	1×10^{-6}
InhR (m^3/d): Inhalation rate	20 (adult); 7.6 (children)
PEF (m^3/kg): Particle emission factor	1.36×109
SA (cm^2): Skin surface that are available for exposure	5700 (adult); 2800 (children)
AF_{soil} (mg/cm^2): Soil to skin adherence factor	0.07 (adult); 0.2(children)

Exposure factors used in estimation for non-carcinogenic risk.

Adapted from USEPA (1997; 2002; 2009; 2013).

Table S4 References dose (RfD) for non-carcinogenic metals and slope factor (SF) for carcinogenic metals.

Exposure pathway		Tl	As	Cd	Cr	Cu	Pb	Zn
RfD (mg/kg/day)	Ingestion	8.00E-05	3.00E-04	1.00E-03	3.00E-03	4.00E-02	3.50E-03	3.00E-01
	Dermal	1.00E-05	1.23E-04	1.00E-05	6.00E-05	1.20E-02	5.25E-04	6.00E-02
	Inhalation	8.00E-05	1.50E−05	1.00E-05	2.86E-05	4.02E-02	3.52E-03	3.00E-01
SF (kg·d/mg)	Ingestion	-	1.50E+00	-	-	-	8.50E-03	-
	Dermal	-	3.66E+00	-	-	-	-	-
	Inhalation	-	1.51E+01	6.30E+00	4.20E+01	-	-	-

Note: E is the abbreviation of exponent, which means the index based on 10.

Adapted from Integrated Risk Information System of the US Environmental Protection Agency (USEPA, 2013).

Table S5 Hazard quotient (HQ) and cumulative hazard index (HI) for non-carcinogenic risk.

	Adults				Children			
Element	HQ_{ing}	HQ_{der}	HQ_{inh}	HI	HQ_{ing}	HQ_{der}	HQ_{inh}	HI
Tl	**5.74E-01**	1.83E-02	8.44E-05	5.92E-01	**4.59E+00**	1.03E-01	1.28E-04	**4.69E+00**
As	**7.42E-01**	**2.17E-01**	**2.18E-03**	9.61E-01	**5.93E+00**	**1.22E+00**	**3.32E-03**	**7.15E+00**
Cd	9.55E-04	3.81E-04	1.40E-05	1.35E-03	7.64E-03	2.14E-03	2.13E-05	9.80E-03
Cr	2.64E-02	5.28E-03	4.08E-04	3.21E-02	2.12E-01	2.96E-02	6.20E-04	2.42E-01
Cu	3.23E-03	4.30E-05	4.73E-07	3.27E-03	2.58E-02	2.41E-04	7.18E-07	2.60E-02
Pb	1.96E-02	5.21E-02	2.86E-06	7.17E-02	1.57E-01	2.92E-01	4.35E-06	4.49E-01
Zn	5.05E-04	1.01E-05	7.43E-08	5.15E-04	4.04E-03	5.66E-05	1.13E-07	4.10E-03
Total	**1.37E+00**	2.93E-01	2.69E-03	**1.66E+00**	**1.09E+01**	**1.65E+00**	4.09E-03	**1.26E+01**

Note: E is the abbreviation of exponent, which means the index based on 10.

Table S6 Carcinogenic risk of adults and children under different exposure pathways.

Element	As	As	As	Cd	Cr	Pb	
Pathway	CR_{Ing}	CR_{der}	CR_{Inh}	CR_{Inh}	CR_{Inh}	CR_{Ing}	TCR
Adults	**1.14E-04**	3.34E-05	1.69E-07	3.03E-10	1.68E-07	2.00E-07	**1.48E-04**
Children	**2.29E-04**	4.69E-05	6.44E-08	1.15E-10	6.38E-08	3.99E-07	**2.76E-04**

Note: E is the abbreviation of exponent, which means the index based on 10.

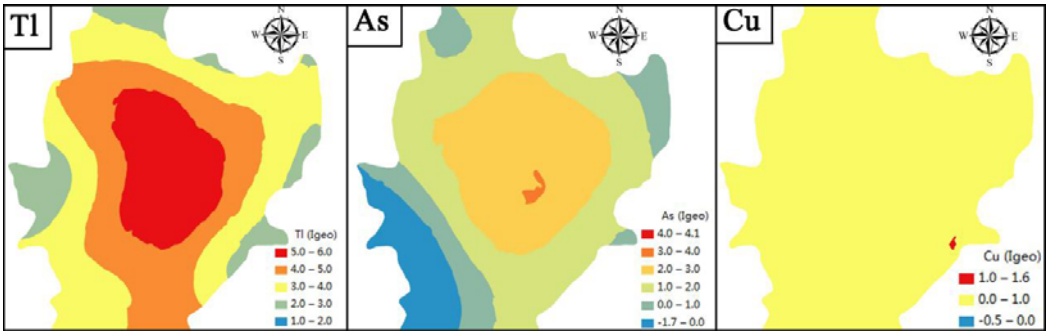

Fig. S1. Geoaccumulation index (I_{geo}) maps of Tl, As and Cu in soil over the study area.

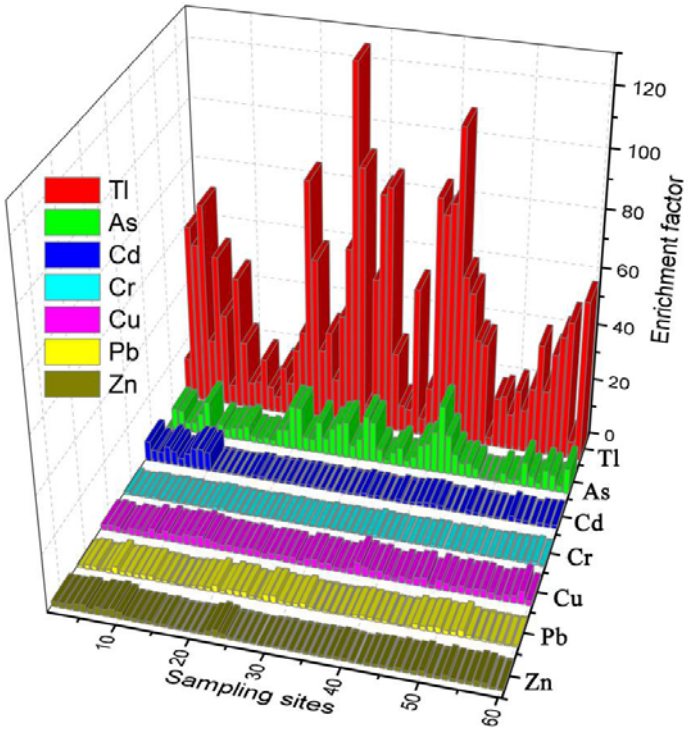

Fig. S2. Enrichment factor of PTEs in river sediment (S1-S10) and topsoil (S11-S60).

References

Hakanson L (1980) An ecological risk index for aquatic pollution control: a sedimentological approach. Water Res 14: 975-1001

USEPA (1997) Exposure factors handbook. EPA/600/P-95/002F. DC: Environmental Protection Agency, Office of Research and Development, Washington

USEPA (2002) Supplemental Guidance for Developing Soil Screening Levels for Superfund Sites, OSWER 9355. Office of Emergency and Remedial Response, Washington

USEPA (2009) Risk assessment guidance for superfund volume i: human health evaluation manual (part F, supplemental guidance for inhalation risk assessment); [EPA/540/R/070/002]

USEPA (2013) Region IX, regional screening levels (formerly PRGs). San Francisco, CA 94105. Available at: http://www.epa.gov/region9/superfund/prg/

Islam MS, Ahmed MK, Raknuzzaman M et al (2015) Heavy metal pollution in surface water and sediment: a preliminary assessment of an urban river in a developing country. Ecol Indic 48: 282-291